Endocytic processing of connexin43 gap junctions: a morphological study

Edward LEITHE[1], Andreas BRECH and Edgar RIVEDAL

Institute for Cancer Research, The Norwegian Radium Hospital, Montebello, N-0310 Oslo, Norway

Gap junctions are plasma membrane areas enriched in channels that provide direct intercellular communication. Gap junctions have a high turnover rate; however, the mechanisms by which gap junctions are degraded are incompletely understood. In the present study, we show that in response to phorbol ester treatment, the gap junction channel protein Cx43 (connexin43) is redistributed from the plasma membrane to intracellular vesicles positive for markers for early and late endosomes and for the endolysosomal protease cathepsin D. Immunoelectron microscopy studies indicate that the double membranes of internalized gap junctions undergo separation and cutting, resulting in multivesicular endosomes enriched in Cx43 protein. Using preloading of BSA–gold conjugates to mark lysosomes, we provide evidence suggesting that the degradation process of the double-membrane structure of annular gap junctions occurs prior to transport of Cx43 to the lysosome. The results further suggest that bafilomycin A1, an inhibitor of vacuolar H^+-ATPases, causes accumulation of Cx43 in early endosomes. Taken together, these findings indicate that internalized gap junctions undergo a maturation process from tightly sealed double-membrane vacuoles to connexin-enriched multivesicular endosomes with a single limiting membrane. The results further suggest that along with the processing of the double-membrane structure of annular gap junctions, connexins are trafficked via early and late endosomes, finally resulting in their endolysosomal degradation.

Key words: bafilomycin A1, connexin43, endocytosis, gap junction, PMA, proteolysis.

INTRODUCTION

Neighbouring cells are able to exchange ions, metabolites and cell-signalling molecules of < 1 kDa via hydrophilic channels composed of proteins called connexins [1]. Connexins are tetramembrane-spanning proteins that oligomerize into hemichannels [2,3]. These hemichannels, each consisting of six connexins, are transported to the plasma membrane and interact with similar structures in the adjacent cells, thereby forming complete intercellular channels [4]. The intercellular channels become densely packed, and the plasma membrane domains enriched in such channels are called gap junctions. Gap junctional intercellular communication plays an important role in cell growth, differentiation and development [5].

One gap junction plaque may contain from only a few to many thousand individual channels [4]. Studies in living cells have revealed that gap junctions are dynamic compartments that drift laterally in the plasma membrane [6,7]. Newly synthesized connexin channels are continually added to the edges of existing gap junctions. From there, they migrate towards the centre of the gap junction, where they are removed by endocytosis [8,9]. Gap junctions have a high turnover rate, and connexins usually have a half-life of 1.5–5 h [10–13]. Regulation of gap junction endocytosis is considered to be an important mechanism for modulating gap junctional intercellular communication [14–16]. A gap junction contains the plasma membranes of two neighbouring cells, which are tightly sealed to each other. During gap junction endocytosis, both membranes are internalized into one of the adjacent cells [17]. The lumen of the resulting double-membrane vacuole thus contains what was previously the cytosol of the neighbouring cell. The internalized gap junction, also called an annular gap junction, is then proteolytically degraded. The intracellular trafficking of connexin proteins after gap junction internalization is incompletely understood. However, both biochemical and morphological studies indicate that lysosomes play an important role in gap junction degradation [15]. Some electron microscopy studies suggest that annular gap junctions fuse directly with lysosomes [18,19]. Others have shown that annular gap junctions sometimes have a complex structure, containing both single- and double-membrane profiles [20–22]. However, our knowledge of the changes in membrane topology that annular gap junctions undergo during their degradation process is still fragmentary.

The connexin protein family consists of > 20 members [23]. Cx43 (connexin43) is ubiquitously expressed in human tissues and is one of the best-studied connexins. Cx43 is often downregulated in cancer cells and has been reported to function as a tumour suppressor protein [24,25]. The tumour-promoting phorbol ester PMA induces a rapid and transient block in Cx43 gap junctional communication in many cell types [26–29]. This block in intercellular communication is often followed by accelerated endocytosis and degradation of Cx43 gap junctions [30,31]. PMA has also been reported to block assembly of gap junctions [32].

The aim of the present study was to gain a better understanding of the endocytic trafficking and degradation process of Cx43 gap junctions. We show that after PMA treatment, Cx43 is transported to early and late endosomes and co-localizes with cathepsin D. Using immunogold electron microscopy, we provide evidence suggesting that annular gap junctions undergo a maturation process from tightly sealed double-membrane vacuoles to Cx43-enriched multivesicular endosomes containing a single limiting membrane. The results further indicate that inhibition of vacuolar H^+-ATPases causes an accumulation of Cx43 in early endosomes.

EXPERIMENTAL

Reagents and antibodies

PMA, EGF (epidermal growth factor), bafilomycin A1 and cycloheximide were obtained from Sigma (St. Louis, MO, U.S.A.). Anti-Cx43 antibodies were obtained by injecting rabbits with a synthetic peptide consisting of the 20 C-terminal amino acids of

Abbreviations used: Cx43, connexin43; DMEM, Dulbecco's modified Eagle's medium; EEA1, early endosome antigen 1; EGF, epidermal growth factor.

[1] To whom correspondence should be addressed (email eleithe@medisin.uio.no).

Cx43 [33]. Mouse anti-Cx43 antibodies were purchased from Chemicon International (Temecula, CA, U.S.A.). Goat anti-Cx43 IgM antibodies recognizing the amino acids 130–143 in the internal loop of Cx43 were obtained from Sigma. Mouse anti-EEA1 (early endosome antigen 1) antibodies were obtained from BD Transduction Laboratories (San Diego, CA, U.S.A.). Mouse anti-rat CD63 antibodies were from BD PharMingen (San Diego, CA, U.S.A.). Goat anti-cathepsin D antibodies were obtained from Santa Cruz Biotechnology (Santa Cruz, CA, U.S.A.). Alexa488-conjugated goat anti-rabbit IgG, Alexa488-conjugated chicken anti-mouse IgG, Alexa594-conjugated goat anti-mouse IgG and Alexa594-conjugated chicken anti-goat IgG antibodies were obtained from Molecular Probes (Eugene, OR, U.S.A.). Goat anti-rabbit IgG secondary antibodies conjugated with horseradish peroxidase were from Bio-Rad (Hercules, CA, U.S.A.). Horseradish peroxidase-conjugated donkey anti-mouse IgM antibodies were obtained from Jackson Immunoresearch Laboratories (West Grove, PA, U.S.A.). Lucifer Yellow was purchased from Sigma.

Cell culture and treatment

The rat liver epithelial cell line IAR20 was obtained from the International Agency for Research on Cancer (Lyon, France). The cells were originally isolated from normal in-bred BD-IV rats and express endogenous Cx43 [34,35]. Cells were grown in DMEM (Dulbecco's modified Eagle's medium) supplemented with 10 % (v/v) fetal bovine serum (Gibco BRL Life Technologies, Inchinnan, U.K.). Cells (1×10^6) were plated on to 60 mm Petri dishes (Costar, Cambridge, MA, U.S.A.) 48 h prior to experiments. The growth medium was replaced with DMEM supplemented with 1 % fetal bovine serum after 24 h.

Determination of gap junctional intercellular communication by quantitative scrape loading

Quantitative scrape loading was performed as described previously [36,37]. Briefly, the confluent cell layer was washed twice with PBS, 0.05 % (w/v) Lucifer Yellow (Sigma) dissolved in PBS without Ca^{2+} and Mg^{2+} was added to this, and the cell layer was cut with a surgical scalpel. After 3.5 min, the Lucifer Yellow solution was removed, and the dishes were rinsed four times in PBS, fixed in 4 % (w/v) formaldehyde in PBS and mounted with a glass coverslip. Digital monochrome images were acquired by a Cohu 4912 CCD (charge-coupled device) camera (Cohu, San Diego, CA, U.S.A.) and a Scion LG-3 frame grabber card (Scion, Frederick, MD, U.S.A.).

Western blotting

Cells were washed with PBS and scraped in 500 μl of SDS electrophoresis sample buffer (10 mM Tris, pH 6.8, 15 %, w/v, glycerol, 3 %, w/v, SDS, 0.01 %, w/v, Bromophenol Blue and 5 %, v/v, 2-mercaptoethanol). The cell lysates were sonicated and heated for 5 min at 95 °C. Samples were separated by SDS/8 % PAGE and transferred on to nitrocellulose membranes as described previously [33]. The blotting membranes were developed with 4-chloro-1-naphthol (Bio-Rad) or chemiluminescence (Cell Signaling Technology). In some experiments, the intensity of Cx43 bands was quantified using Scion Image (Scion). Statistically significant differences between samples were identified using ANOVA with Tukey–Kramer multiple comparisons test.

Immunofluorescence microscopy

The IAR20 cell monolayer was fixed with 4 % formaldehyde in PBS for 30 min at room temperature, rinsed in PBS and permeabilized with 0.1 % Triton X-100. Cells were incubated first with PBS containing 5 % (w/v) dried milk and 0.1 % Tween 20 for 1 h and subsequently with primary antibodies for 1 h, washed with PBS and incubated with Alexa-conjugated secondary antibodies for 1 h. The cells were mounted with Mowiol medium. Immunofluorescence images were captured using a Nikon E800 microscope with a Spot-2 camera. For co-localization studies, cells fixed on coverslips were examined in a Leica TCS-NT laser confocal microscope. Image processing was performed with Adobe Photoshop version 7.0.

Preparation of colloidal gold protein conjugates

Colloidal gold particles were prepared as described previously [38]. Solutions containing 8 nm colloidal gold particles were complexed with BSA as described in [39]. Aggregates were removed by centrifugation at 16000 rev./min for 25 min in a J2-21 Beckman centrifuge equipped with a JA-20 rotor. BSA–gold was subsequently recovered by centrifugation of the supernatant at 35000 rev./min for 40 min in a Beckman L8-80 ultracentrifuge equipped with a 60Ti rotor.

Immunoelectron microscopy

Cells were incubated with 8 nm BSA–gold for 10 min to identify early endosomes, or for 30 min to identify both early and late endosomes. To identify lysosomes, cells were incubated with 8 nm BSA–gold for 3 h and chased overnight. Cells were treated as indicated and fixed in 4 % formaldehyde and 0.1 % glutaraldehyde in 0.1 M PHEM buffer (120 mM Pipes, 50 mM Hepes, 20 mM EGTA and 4 mM $MgCl_2$, pH 7.4) for 2 h, washed and scraped in PBS supplemented with 1 % gelatin. Cells were collected by centrifugation and the pellet was embedded with 10 % (w/v) gelatin in PBS. The cell pellet was incubated in 2.3 M sucrose overnight at 4 °C, mounted and frozen in liquid nitrogen. Ultrathin cryosections were cut at − 110 °C with a diamond knife in an Ultracut microtome (Leica), and collected and thawed on 2.3 M sucrose. Sections were transferred to formvar/carbon-coated grids and labelled with anti-Cx43 antibodies followed by Protein A–gold conjugates (obtained from G. Posthuma and J. W. Slot, University Medical Center, Utrecht, The Netherlands) as described previously [40]. The labelled cryosections were examined with a Philips CM10 electron microscope.

RESULTS

PMA induces relocalization of Cx43 from the plasma membrane to intracellular vesicles positive for markers for early and late endosomes and cathepsin D

PMA has two major effects on Cx43 gap junctions in IAR20 cells. The first is a rapid and nearly complete inhibition of gap junctional intercellular communication (Figure 1A) [36]. The second is a dramatic acceleration of the gap junction endocytosis rate. After 30 min of PMA treatment, nearly all Cx43 gap junctions are lost from the plasma membrane, and Cx43 is localized in intracellular vesicles (Figure 1A) [30]. As a first approach to study the endocytic trafficking of Cx43 gap junctions, the localization of Cx43 in relation to known endocytic markers was examined by confocal immunofluorescence microscopy. EEA1 is localized on early endosomes and is involved in homotypic fusion between early endosomes [41]. After 30 min of PMA treatment, Cx43 often

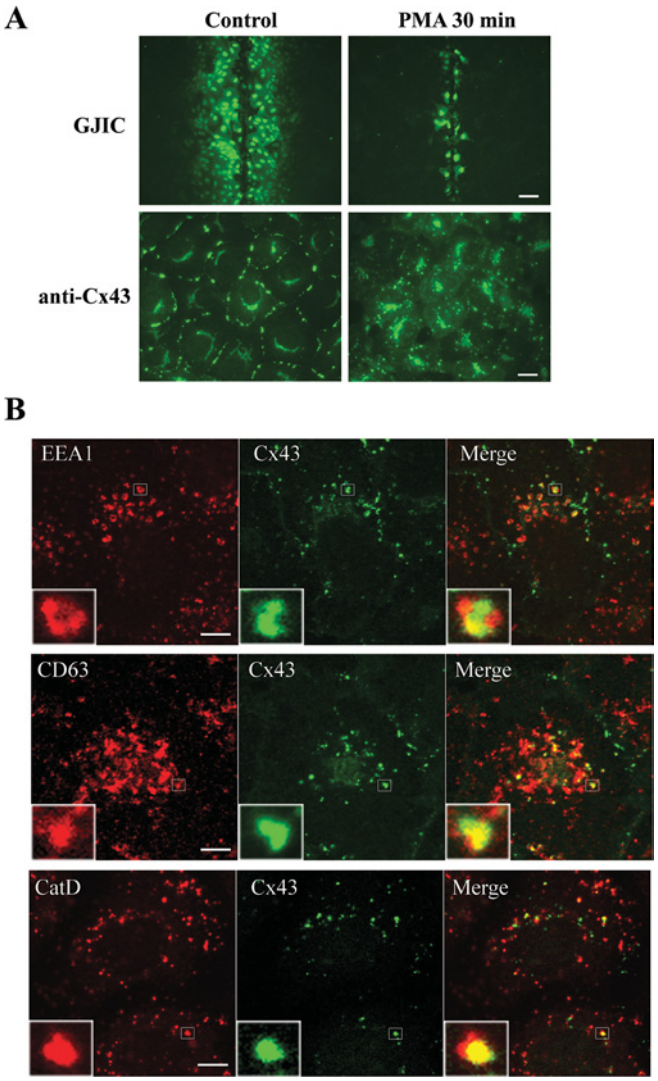

Figure 1 Immunofluorescence analysis of PMA-induced endocytosis of Cx43

(**A**) IAR20 cells were left untreated or treated with PMA (100 ng/ml) for 30 min. Gap junctional intercellular communication (GJIC) was examined by scrape loading of cells with Lucifer Yellow (upper panels; scale bar, 100 μm). Control IAR20 cells have extensive dye coupling, whereas PMA causes a nearly complete inhibition of dye transfer between cells. Cells were fixed, immunostained with anti-Cx43 antibodies and visualized using immunofluorescence microscopy (lower panels; scale bar, 20 μm). PMA causes redistribution of Cx43 from the plasma membrane to intracellular vesicles. (**B**) Cells were treated with PMA (100 ng/ml) for 30 min. Cells were fixed, double-stained with Cx43 antibody (middle panels) and EEA1, CD63 or cathepsin D antibody (left panels) as indicated and then visualized using confocal immunofluorescence microscopy. Merged images are shown in the right panels, with yellow indicating co-localization. Insets show enlarged view of representative Cx43-positive endosomes. Scale bars, 10 μm.

localized in EEA1-positive endosomes (Figure 1B). In agreement with previous studies, EEA1 localized in special microdomains of the endosome [42]. Interestingly, Cx43 also often appeared to localize in microdomains of early endosomes. The Cx43 microdomains appeared to be distinct from the EEA1 microdomains. The tetraspanin CD63 is localized in late endosomes and lysosomes [43]. Internalized Cx43 was often found to localize in vesicles positive for CD63, indicating that Cx43 is transported from early to late endosomes and lysosomes. Cathepsin D is an aspartic endoprotease that has previously been reported to be localized within the endolysosomal system [44]. After PMA treatment for 30 min, some Cx43-positive vesicles were devoid of cathepsin

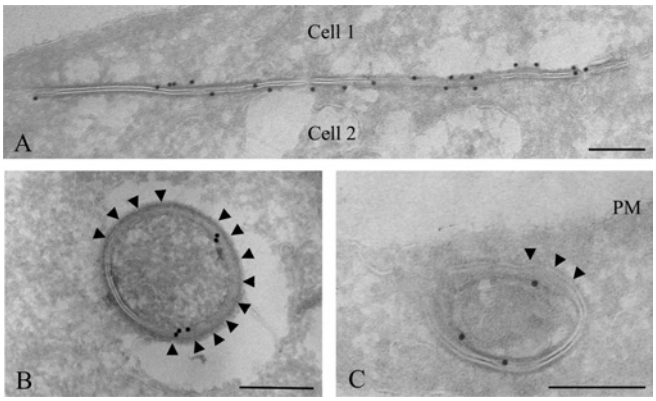

Figure 2 Immunoelectron microscopy of intercellular and annular Cx43 gap junctions

To identify lysosomes, cells were incubated with 8 nm BSA–gold for 3 h and chased overnight. Cells were left untreated or treated with PMA (100 ng/ml) for 30 min and fixed. Cryosections of untreated cells (**A**) or cells treated with PMA (100 ng/ml) for 30 min (**B**, **C**) were labelled for Cx43 (15 nm gold). (**A**) In untreated cells, Cx43 gap junction plaques were frequently observed between adjacent cells. (**B**, **C**) Annular gap junctions. Large areas of the gap junction double membranes appear to have started to separate (arrowheads). PM, plasma membrane. Scale bars, 200 nm.

D, while in other vesicles there was co-localization between Cx43 and cathepsin D, suggesting that a subpopulation of Cx43 had reached the lysosomes (Figure 1B). Together, these results indicate that Cx43 is transported to early endosomes in response to PMA treatment. This is followed by transport to late endosomes and lysosomes. We have previously shown that EGF induces endocytosis of Cx43 in IAR20 cells [45]. Also in response to EGF, Cx43 co-localized with EEA1, CD63 and cathepsin D, indicating that this trafficking pattern of Cx43 is not specifically induced by PMA (results not shown).

Immunoelectron microscopic evidence suggesting that internalized gap junctions undergo a maturation process to form multivesicular endosomes

In order to investigate the degradation process of Cx43 annular gap junctions with sufficient resolution to reveal the gap junction membrane topology, immunoelectron microscopy was performed. To identify lysosomes, cells were grown in a medium containing 8 nm BSA–gold conjugates for 3 h, followed by a 24 h chase. Under these conditions, the gold particles are taken up by endocytosis and accumulate in lysosomes [46]. The cells were subsequently left untreated or treated with PMA and fixed for electron microscopy. Cryosections of the cells were immunogold-labelled for Cx43. In accordance with the immunofluorescence data, control IAR20 cells were frequently found to have gap junction plaques at the plasma membrane between neighbouring cells (Figure 2A). Cells treated with PMA for 30 min were often found to have Cx43 labelling in intracellular vesicular structures. Some of these vesicles contained two tightly apposed membranes similar to the double membranes in intercellular gap junctions and are, in accordance with previous studies, here defined as annular gap junctions (Figures 2B and 2C). Annular gap junctions have previously been shown to be internalized gap junctions [17]. Sometimes, large areas of the annular gap junction double membrane appeared to have started to separate (Figures 2B and 2C). Importantly, membranes of gap junctions sometimes appeared to be cut and to form small single-membrane vesicles (Figures 3A and 3B). These vesicles were similar, both in size and shape, to the vesicles usually seen inside multivesicular endosomes [47]. Cx43

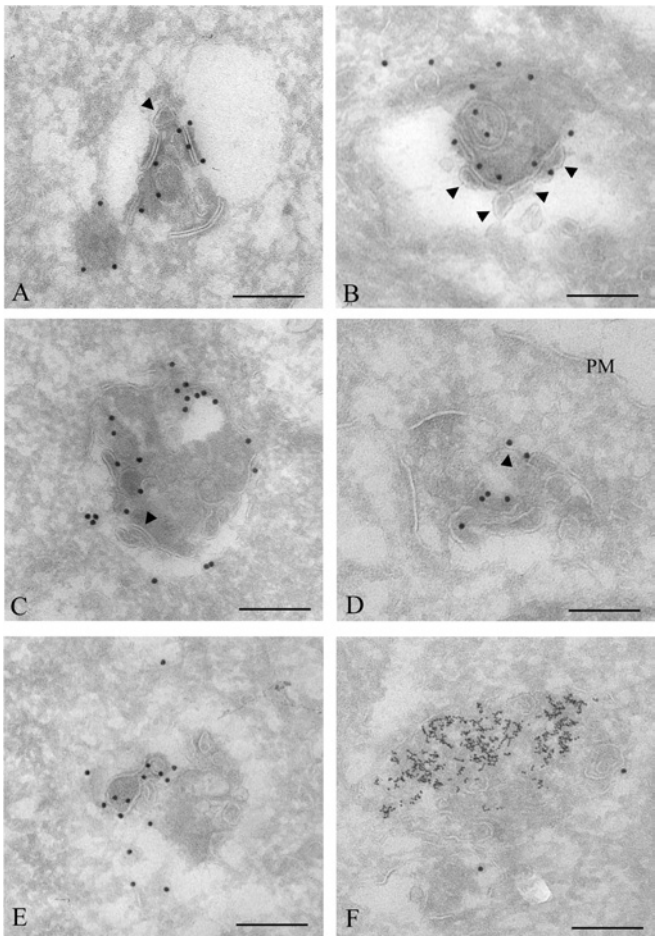

Figure 3 Immunoelectron microscopy analysis of PMA-induced Cx43 gap junction degradation

To identify lysosomes, cells were incubated with 8 nm BSA–gold for 3 h and chased overnight. Cells were treated with PMA (100 ng/ml) for 30 min, fixed, prepared for electron microscopy and labelled for Cx43 (15 nm gold). (**A**) An annular gap junction appears to have started to be cut into smaller membrane pieces. Some parts of the gap junction membrane appear to form a small intravacuolar vesicle (arrowhead). (**B**) The double membrane of the annular gap junction appears to be cut and to separate. The resulting single membranes appear to form small vesicles (arrowheads), similar to vesicles inside multivesicular endosomes. (**C**–**E**) Cx43 labelling in multivesicular endosomes. Some of the intravacuolar vesicles have irregular shapes and are different from vesicles usually seen in multivesicular endosomes. Some membrane areas of the endosomes appear to be remnants of double-membrane gap junctions (arrowheads). (**F**) Cx43 labelling in a lysosome, identified as an electron-dense vesicle containing endocytosed 8 nm gold particles. PM, plasma membrane. Scale bars, 200 nm.

was also localized to multivesicular endosomes, many of which appeared to contain partly degraded gap junction membrane areas (Figures 3C–3E). Taken together, these results indicate that during their endocytosis, the two membranes of annular gap junctions are separated into two single membranes. Parts of these membranes are cut and form small vesicles, finally resulting in Cx43-enriched multivesicular endosomes.

Importantly, the annular gap junctions that had started their degradation process were devoid of 8 nm gold, indicating that their degradation process starts prior to fusion with lysosomes. Cx43 labelling was sometimes found in lysosomes, defined as electron-dense vacuoles containing 8 nm gold particles (Figure 3F). However, we did not observe annular gap junctions fusing with lysosomes, or fragments of annular gap junctions in lysosomes. These results suggest that annular gap junctions are transformed into multivesicular endosomes before Cx43 is delivered to lysosomes. Annular gap junctions that had started their degradation process were in general labelled with more gold particles than intact annular gap junctions. This was possibly due to increased accessibility of the anti-Cx43 antibody to the C-terminal tail of Cx43 as a result of partial processing of the gap junction double membrane. Cells treated with PMA for 60 min showed little Cx43 labelling, both in multivesicular endosomes and lysosomes (results not shown). This observation is in agreement with previous studies showing that prolonged PMA treatment causes Cx43 degradation in IAR20 cells [30].

The above findings indicate that annular gap junctions, consisting of two tightly apposed membranes, are processed to vacuoles consisting of single limiting membranes and many internal vesicles. To investigate whether such a splitting of the two membranes and formation of small intraendosomal vesicles are specific to PMA treatment, cells were treated with EGF, which has previously been shown to induce endocytosis of Cx43 in IAR20 cells [45]. Separation of the two membranes of gap junctions and formation of small Cx43-containing intravacuolar vesicles were also observed in EGF-treated cells (Figures 4A–4F). Occasionally, annular gap junctions appeared to fuse with endosomes (Figure 4B). Also, in control IAR20 cells, Cx43 was sometimes found to be organized as annular gap junctions or localized in multivesicular bodies (results not shown). Together, these results indicate that the processing of annular gap junctions into multivesicular endosomes is part of the normal life cycle of Cx43, and is not specific to PMA treatment.

Immunoelectron microscopic evidence suggesting that Cx43 is transported to early and late endosomes following PMA treatment

Since the immunofluorescence data showed localization of internalized Cx43 in vesicles positive for markers for early and late endosomes, we wanted to examine the localization of internalized Cx43 in relation to early and late endosomes at the electron microscopic level. Previous studies have shown that when cells are incubated with BSA–gold for 10 min, internalized BSA–gold localizes in early endosomes [48,49]. Thus, to investigate the localization of internalized Cx43 in relation to early endosomes, IAR20 cells were treated with PMA for a total of 30 min, with 8 nm BSA–gold present in the growth medium for the last 10 min. Cells were then fixed for electron microscopy and immunogold-labelled against Cx43. As expected, under these conditions, 8 nm BSA–gold was found in electron-lucent vacuoles containing only a few internal vesicles, and morphologically similar to early endosomes. Cx43 was frequently found to localize in vacuoles containing 8 nm gold (Figures 5A and 5B). Some of these vacuoles were morphologically similar to early endosomes. Others appeared to have the characteristics of both early endosomes and annular gap junctions and are possibly hybrid organelles between these two types of vacuoles.

After a 30 min incubation, internalized BSA–gold localizes in both early and late endosomes [50]. Thus, to examine the localization of endocytosed Cx43 in relation to late endosomes, cells were co-incubated with PMA and 8 nm BSA–gold for 30 min. As expected, under these conditions, BSA–gold was not only found to localize in early endosomes, but also in vacuoles with a more globular shape than early endosomes and containing more internal vesicles. These vacuoles were, in accordance with previous studies, defined as late endosomes. By immunogold labelling, Cx43 was found to localize in these vacuoles (Figures 5C and 5D). These observations are in accordance with the immunofluorescence microscopy studies and indicate that Cx43 is transported to early and late endosomes after its PMA-induced internalization. Taken together, the electron microscopy data reveal two major events

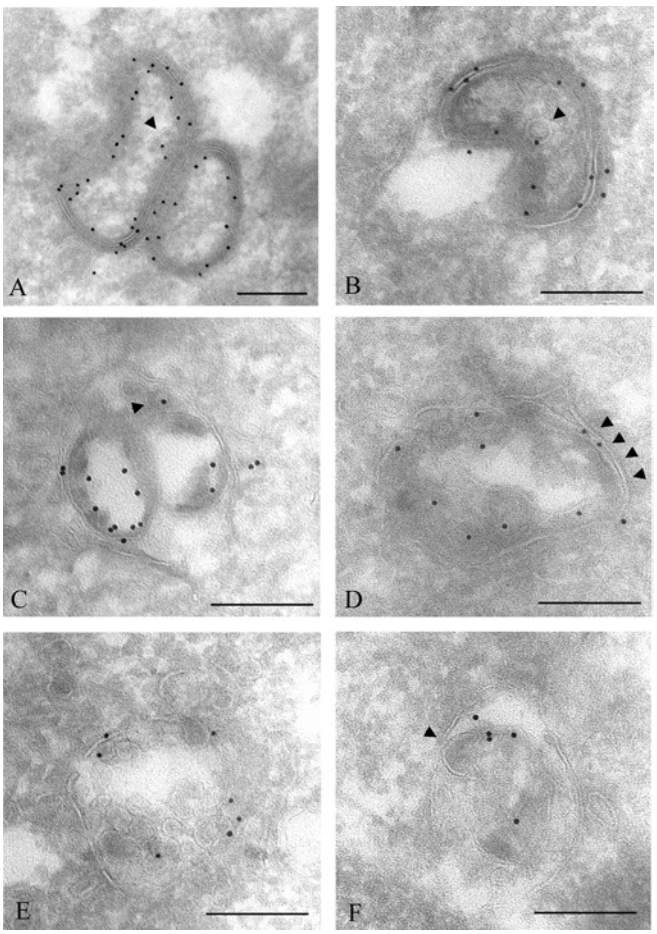

Figure 4 Immunoelectron microscopy analysis of EGF-induced Cx43 gap junction degradation

IAR20 cells were treated with EGF (50 ng/ml) for 30 min. The cells were fixed, prepared for electron microscopy and labelled for Cx43 (10 nm gold). (**A**) Two tightly apposed annular gap junctions. Some parts of the double membranes appear to have started to separate. One single-membrane vesicle inside the annular gap junction is labelled with one gold particle (arrowhead). (**B**) An annular gap junction appears to fuse with an endosome. The annular gap junction appears to invaginate into itself. One single-membrane vesicle inside the annular gap junction is labelled with one gold particle (arrowhead). (**C**) An annular gap junction containing two large and one small (arrowhead) internal vesicles with Cx43 labelling. At some places, the vesicles appear to be tightly sealed with the outer membrane, similar to what is observed between the two membranes of gap junctions. (**D**–**F**) Cx43 is localized in multivesicular endosomes. Some of the intravacuolar vesicles have irregular shapes and are different from vesicles usually seen in multivesicular endosomes. Some of the vesicles are tightly associated with the outer membrane, forming double membranes that appear to be remnants of gap junctions (arrowheads). Scale bars, 200 nm.

in the endocytic processing of annular gap junctions. The first is maturation of the double-membrane annular gap junction into a multivesicular endosome with a single limiting membrane. The second event, which appears to occur simultaneously with the processing of the annular gap junction into a multivesicular endosome, is trafficking of Cx43 to early endosomes, probably as a result of direct fusion between annular gap junctions and early endosomes.

Functional vacuolar H^+-ATPases are required for efficient transport of Cx43 from early to late endosomes

The results presented above are consistent with a model in which annular gap junctions are integrated with early and late endosomes. To examine gap junction endocytosis further, it was of interest to elucidate how the endocytic trafficking of Cx43 is affected by inhibition of endosomal acidification. Previous studies have shown that weak bases block Cx43 degradation, indicating that endosomal acidification is required for Cx43 degradation [14]. However, it is not known at which stage in the degradation process of annular gap junctions endosomal acidification is required. To examine this, we used bafilomycin A1, a specific inhibitor of vacuolar H^+-ATPases, to avoid potential unspecific effects of weak bases on Cx43 endocytosis. In agreement with previous studies, PMA treatment for 60 min caused a strong loss of Cx43 gap junctions, as determined by fluorescence microscopy. Under this condition, most of the Cx43 was found in the Golgi region, and the Cx43 signal was strongly reduced when compared with control cells (Figure 6A). In contrast, if cells were incubated with bafilomycin A1 prior to PMA treatment, large amounts of Cx43 were found in intracellular vesicles. Similar results were obtained when PMA was preincubated with concanamycin A, another inhibitor of vacuolar H^+-ATPases (results not shown).

To evaluate further the effect of bafilomycin A1 on PMA-induced Cx43 endocytosis, the Cx43 protein level was examined by Western blotting. In SDS/PAGE, Cx43 usually forms three distinct bands, representing different phosphorylation states of the protein [51]. In agreement with the immunofluorescence data, PMA treatment for 60 min caused a strong loss of Cx43 protein as determined by using an antibody raised against the C-terminal tail of Cx43 (Figure 6B) [30]. This PMA-induced Cx43 degradation of Cx43 was significantly counteracted by bafilomycin A1. To investigate whether bafilomycin A1 affects the degradation of the C-terminal tail of Cx43 differently than the rest

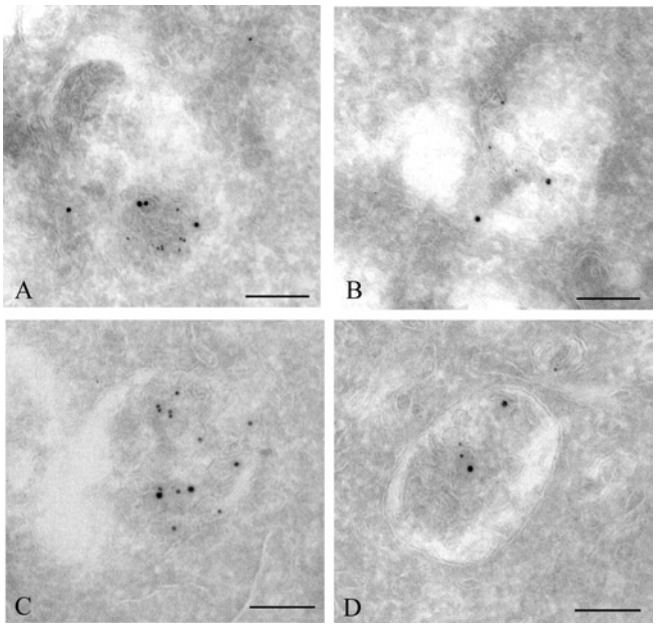

Figure 5 Immunoelectron localization of Cx43 in early and late endosomes

(**A**, **B**) IAR20 cells were treated with PMA (100 ng/ml) for 30 min. During the last 10 min of incubation, 8 nm BSA–gold particles were added to the medium, to mark early endosomes. Cells were fixed, prepared for electron microscopy and labelled for Cx43 (15 nm gold). Early endosomes, characterized by their electron-lucent appearance, a few internal vesicles and content of 8 nm gold particles, were often found to contain Cx43. Cx43 was found both on the limiting vacuolar membrane and on intravacuolar vesicles. (**C**, **D**) To mark both early and late endosomes, cells were treated with PMA (100 ng/ml) for 30 min in a medium containing 8 nm BSA–gold particles. Cells were fixed and labelled for Cx43 (15 nm gold). Cx43 was found in late endosomes, differentiated from early endosomes by their globular form, their more electron-dense appearance and by containing more internal vesicles. Scale bars, 200 nm.

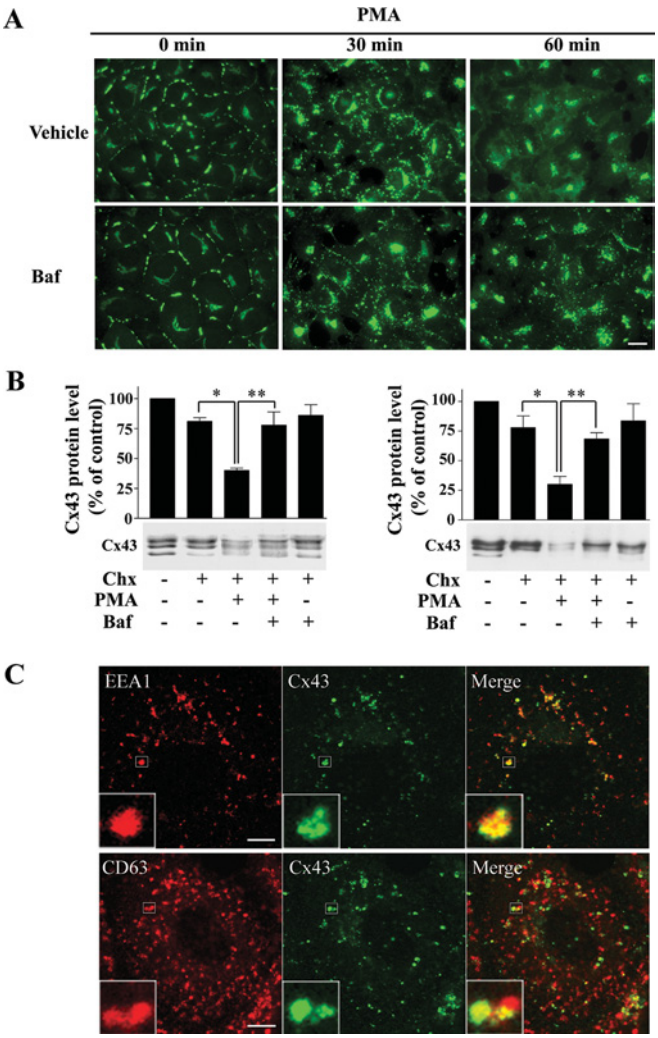

Figure 6 Effect of bafilomycin A1 on PMA-induced endocytosis of Cx43

(**A**) IAR20 cells were treated with bafilomycin A1 (Baf; 200 nM) or vehicle (DMSO) for 30 min prior to and during treatment with PMA (100 ng/ml) for the indicated times. Cells were fixed, immunostained with anti-Cx43 antibodies and visualized using fluorescence microscopy. Scale bar, 20 μm. (**B**) IAR20 cells were left untreated or treated with bafilomycin A1 (200 nM) or vehicle (DMSO) for 30 min prior to and during treatment with PMA (100 ng/ml) and cycloheximide (Chx; 10 μg/ml) or cycloheximide alone for 60 min as indicated. Cell lysates were prepared and equal amounts of total cell protein were subjected to SDS/PAGE. Cx43 was detected by Western blotting using antibodies raised against the C-terminal end of Cx43 (left panel) or antibodies recognizing the amino acids 130–143 in the internal loop of Cx43 (Sigma antibody; right panel). For both antibodies, the Cx43 band intensities on gels were measured using Scion Image. Results shown are the means $\pm$ S.E.M. for three independent experiments. Statistical analysis was performed using one-way ANOVA with Tukey–Kramer multiple comparisons test. Cells treated with cycloheximide and PMA had significantly reduced levels of Cx43 protein compared with cells treated with cycloheximide alone ($^*P < 0.05$). This loss of Cx43 was significantly counteracted by bafilomycin A1 ($^{**}P < 0.05$). (**C**) IAR20 cells were treated with bafilomycin A1 (200 nM) for 30 min prior to and during treatment with PMA (100 ng/ml) for 60 min. Cells were fixed and double stained with Cx43 (middle panels) and EEA1 or CD63 (left panels) antibodies as indicated and visualized using confocal immunofluorescence microscopy. Merged images are shown in the right panels, with yellow indicating co-localization. Insets show enlarged view of representative Cx43-positive endosomes. Scale bars, 10 μm.

of the Cx43 protein, Western blotting was performed with an antibody that recognizes the intracellular loop of Cx43. Also by these experiments, bafilomycin A1 was found to counteract the PMA-induced loss of Cx43 protein (Figure 6B). Similar results were obtained when PMA was preincubated with concanamycin A (results not shown). Together, these results indicate that functional vacuolar H^+-ATPases are required for efficient endocytic trafficking and degradation of Cx43.

To examine at which stage in Cx43 endocytosis functional vacuolar H^+-ATPases are required, cells preincubated with bafilomycin A1 prior to PMA treatment for 60 min were examined by confocal immunofluorescence microscopy. Under these conditions, most of the Cx43-containing vesicles were EEA1-positive, although some Cx43 was also found in vesicles positive for CD63 (Figure 6C). These results indicate that functional vacuolar H^+-ATPases are a prerequisite for efficient transport of Cx43 from early to late endosomes.

We next examined the effect of bafilomycin A1 on Cx43 endocytosis by electron microscopy. To identify lysosomes, cells were grown in a medium containing 8 nm BSA–gold conjugates for 3 h, followed by a 24 h chase. The cells were then pretreated with bafilomycin A1 and added PMA for 60 min. Cells were fixed for electron microscopy and immunogold-labelled for Cx43. In accordance with the immunofluorescence microscopy observations, Cx43 labelling was, under these conditions, strongly enhanced compared with cells treated with PMA alone. Cx43 was mostly found in multivesicular structures, some of which resembled early endosomes (Figures 7A and 7B). Cx43 was also found in more electron-dense endosomes, often containing several intraendosomal vesicles (Figures 7C and 7D). Sometimes, these vacuoles contained what appeared to be remnants of gap junction double membranes. Importantly, most of the Cx43-positive vesicles were devoid of 8 nm gold, indicating that bafilomycin A1 inhibits endocytic trafficking of Cx43 before Cx43 enters lysosomes. Taken together, these results are in line with the immunofluorescence studies and indicate that endosomal acidification is required for Cx43 endocytosis at early stages, prior to transport of Cx43 to lysosomes. We occasionally observed Cx43-positive multivesicular endosomes that appeared to fuse with lysosomes (Figure 7E). These observations are in accordance with our hypothesis that annular gap junctions mature into multivesicular endosomes prior to transport of Cx43 to lysosomes. We also sometimes observed Cx43 labelling in enlarged multivesicular endosomes containing 8 nm gold particles (Figure 7F). Similar vacuoles were observed in cells treated only with PMA (results not shown). Possibly, these endosomes represent hybrid organelles between late endosomes and lysosomes (see the Discussion section).

DISCUSSION

In the present study, the endocytic processing of Cx43 gap junctions was examined using confocal immunofluorescence microscopy and immunoelectron microscopy. While Cx43 was localized in gap junctions between adjacent cells in control IAR20 cells, most of the Cx43 localized in intracellular vacuoles following PMA treatment. Sometimes, annular gap junctions in which the double membrane had started splitting were observed. The gap junction membranes further appeared to form intraendosomal, single-membrane vesicles similar to vesicles found inside multivesicular endosomes. Based on these observations, we propose that annular gap junctions undergo a maturation process and are transformed into single-membrane multivesicular endosomes enriched in connexin proteins. Simultaneously with this processing of the annular gap junctions into vacuoles with a single limiting membrane, the results suggest that Cx43 is transported to early endosomes, possibly as a result of direct fusion between annular gap junctions and early endosomes.

The observation that the double membrane of annular gap junctions might separate is in accordance with previous studies in other cell types [20,21]. Annular gap junctions have also been

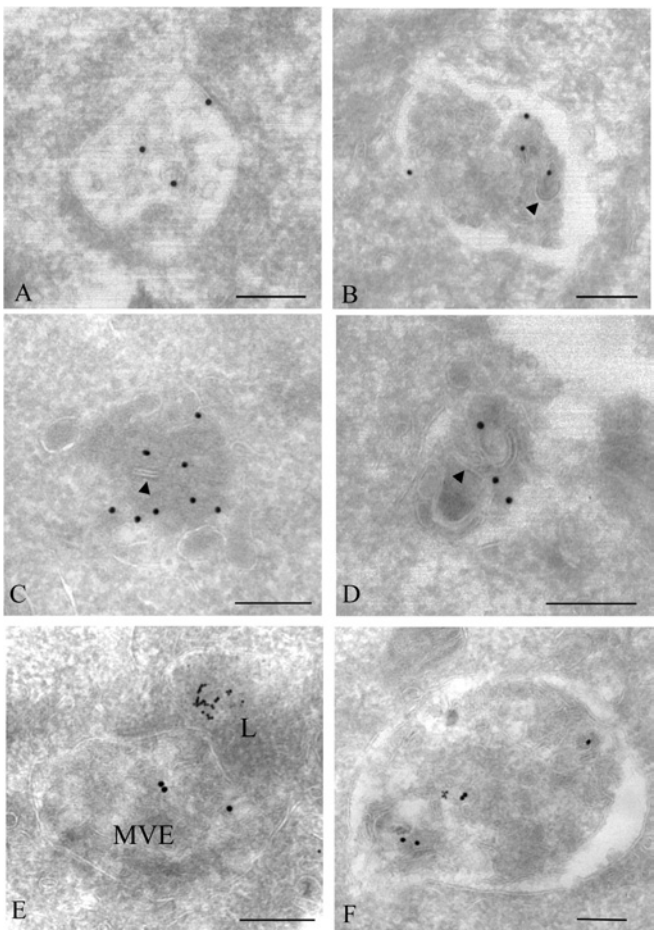

Figure 7 Immunoelectron microscopy analysis of Cx43 localization in cells treated with bafilomycin A1 and PMA

To identify lysosomes, cells were incubated with 8 nm BSA–gold for 3 h and chased overnight. IAR20 cells were treated with bafilomycin A1 (200 nM) for 30 min prior to and during treatment with PMA (100 ng/ml) for 60 min, fixed, prepared for electron microscopy and labelled for Cx43 (15 nm gold). (**A**) Cx43 often localized in electron-lucent vacuoles with few internal vesicles, which resembled early endosomes. Cx43 was, under these conditions, found both on the limiting membrane of the vacuole and on the internal vesicles. (**B**–**D**) Cx43 was also found in more electron-lucent vacuoles containing several internal vesicles. Sometimes these vacuoles contained what appeared to be remnants of gap junction double membranes (arrowheads). (**E**) Cx43 labelling in multivesicular endosome that appear to fuse with a lysosome. (**F**) Cx43 labelling in enlarged multivesicular endosome with 8 nm gold particles. Scale bars, 200 nm.

reported to be able to form complex membrane profiles containing both single and double bilipid layers [20–22]. The origin of these single membranes inside the annular gap junction was, however, not clear. In the present analysis, we have shown that the single-membrane vesicles inside annular gap junctions contain connexin protein. The present study further provides evidence suggesting that the single-membrane vesicles inside annular gap junctions are derived from splitting and cutting of the annular gap junction double membrane. In light of the present study, the complex annular gap junctions that have been described in previous studies might represent annular gap junctions that have started their processing into a multivesicular endosome [20–22].

By immunofluoresence microscopy, internalized Cx43 was found to localize in CD63-positive vesicles, a marker for late endosomes and lysosomes. Immunofluorescence data show that Cx43 endocytosis starts approx. 10 min after PMA treatment, and new gap junctions are continually being internalized until approx. 45 min of PMA treatment (results not shown). Thus the endocytosis of Cx43 gap junctions in response to PMA treatment is not synchronized, which is reflected in the results showing that Cx43 localizes to both early and late endosomes after 30 min of PMA treatment. Internalized Cx43 also sometimes localizes in cathepsin D-enriched endosomal compartments. To the best of our knowledge, this is the first demonstration of co-localization between a connexin and a lysosomal protease. The transport of Cx43 to late endosomes and lysosomes is also supported by the electron microscopy data. Together, these observations indicate that annular gap junction-derived multivesicular endosomes follow the standard trafficking route of endosomes and are able to fuse with lysosomes. Previous studies in other cell types have suggested that annular gap junctions are able to fuse directly with lysosomes [18,19]. In contrast with these studies, we did not observe annular gap junctions fusing with lysosomes. Neither did we observe fragments of gap junctions localized in lysosomes. Internalized gap junctions therefore appear to be able to follow two alternative and distinct endocytic pathways: one involving direct fusion between annular gap junctions and lysosomes and the other involving a maturation process of annular gap junctions into multivesicular endosomes, which subsequently fuse with lysosomes. Probably, there are cell-specific variations with regard to which endocytic pathway is used in the degradation of gap junctions. However, it must be taken into consideration that without specific labelling, it might be difficult to differentiate between the various vacuoles involved in endocytic transport. In the present study, in which lysosomes could be efficiently differentiated from late endosomes by the uptake of BSA–gold, the degradation processing of the gap junction double membrane into single membranes was found to occur prior to fusion with lysosomes. It should, however, be noted that, although we did not observe annular gap junctions fusing with dense core lysosomes, we cannot rule out that this occurs in IAR20 cells.

Although lysosomes sometimes were found to contain Cx43, most of the lysosomes were devoid of Cx43 labelling. Possibly, this low labelling in lysosomes might be due to rapid degradation of Cx43 after fusion between late endosomes and lysosomes. Alternatively, the low Cx43 labelling in lysosomes might reflect that most of the Cx43 is degraded in a hybrid organelle between late endosomes and lysosomes, rather than in lysosomes. There is accumulating evidence indicating that the main function of lysosomes is to store acidic proteases, while the bulk of degradation of endocytosed proteins occurs in hybrid organelles between late endosomes and lysosomes [46]. In this scenario, lysosomes would periodically fuse with late endosomes and form hybrid organelles in which Cx43 degradation occurs. It is also possible that most of the Cx43 is degraded in late endosomes prior to fusion with lysosomes. Indeed, several proteases are localized in early and late endosomes, which could be involved in partial or complete degradation of Cx43 [44]. An important subject for future studies will be to define the endolysosomal proteases involved in Cx43 degradation as well as to determine at which stage in the endocytosis Cx43 degradation occurs.

Previous studies using weak bases indicate that endosomal acidification is a prerequisite for degradation of Cx43 gap junctions [15]. However, it is not known at which stage in Cx43 endocytosis acidification is required. Furthermore, weak bases may have additional effects than counteracting endosomal acidification. Bafilomycin A1 is a specific inhibitor of vacuolar H^+-ATPases and neutralizes acidic organelles [52]. In the present study, we found that bafilomycin A1 strongly counteracted PMA-induced endocytic trafficking of Cx43. In line with this observation, bafilomycin A1 counteracted the PMA-induced Cx43 degradation. Under these conditions, most of the Cx43 localized in early endosomes. However, Cx43 was also partly localized in

CD63-positive vesicles, suggesting that the block in Cx43 trafficking from early to late endosomes was not complete. Together, these results indicate that vacuolar H^+-ATPases are required for efficient trafficking of Cx43 from early to late endosomes. Interestingly, a previous study showed that cells transfected with a mutant subunit of vacuolar H^+-ATPases showed redistribution of Cx43 from the plasma membrane to an intracellular localization [53]. This redistribution of Cx43 was associated with a loss in gap junctional communication [53].

Although the immunofluorescence microscopy studies suggest that most of the Cx43 is localized at the plasma membrane in control cells, it is likely that a subpopulation of Cx43 is localized in early and late endosomes in control cells. Indeed, by electron microscopy, Cx43 was sometimes found to localize in early and late endosomes in untreated cells (results not shown). Given the role of early endosomes as pivotal sorting stations for endocytosed proteins, the finding that Cx43 is transported to early endosomes might have significant physiological relevance. For instance, it opens the possibility that a subpopulation of Cx43 is constitutively recycled to the plasma membrane after internalization. Interestingly, a pool of the major component of adherens junctions, E-cadherin, is continually recycled from early endosomes to the plasma membrane. This recycling has been suggested to be a mechanism for regulating the availability of E-cadherin for junction formation in development, tissue remodelling and tumorigenesis [54]. Importantly, redistribution of Cx43 from the plasma membrane to early endosomes was recently reported to be an early event in the carcinogenesis of Leydig cells [55]. Possibly, impaired endocytic trafficking of Cx43 might be involved in reducing gap junctional communication during tumour development.

In conclusion, the present study indicates that following PMA-induced internalization of Cx43 gap junctions, annular gap junctions are subjected to a maturation process, forming Cx43-enriched multivesicular endosomes. Concomitantly with this processing of the gap junction double membranes, the annular gap junctions integrate with early endosomes. These annular gap junction-derived vacuoles then follow the standard trafficking route of multivesicular endosomes, finally resulting in connexin degradation by endolysosomal proteases. The results further indicate that trafficking of Cx43 from early to late endosomes requires functional vacuolar H^+-ATPases.

We thank Dr Jahn Nesland (Norwegian Radium Hospital, Oslo, Norway) for providing excellent electron microscopy facilities. We are grateful to Ellen Hellesylt and Astri Nordahl for expert technical assistance and to Dr Tore Sanner (Norwegian Radium Hospital, Oslo, Norway) for a critical reading of this paper. This work was supported by The Research Council of Norway and The Norwegian Cancer Society.

REFERENCES

1 Saez, J. C., Berthoud, V. M., Branes, M. C., Martinez, A. D. and Beyer, E. C. (2003) Plasma membrane channels formed by connexins: their regulation and functions. Physiol. Rev. **83**, 1359–1400
2 Musil, L. S. and Goodenough, D. A. (1993) Multisubunit assembly of an integral plasma membrane channel protein, gap junction connexin43, occurs after exit from the ER. Cell (Cambridge, Mass.) **74**, 1065–1077
3 Sosinsky, G. E. (1996) Molecular organization of gap junction membrane channels. J. Bioenerg. Biomembr. **28**, 297–309
4 Segretain, D. and Falk, M. M. (2004) Regulation of connexin biosynthesis, assembly, gap junction formation, and removal. Biochim. Biophys. Acta **1662**, 3–21
5 Wei, C. J., Xu, X. and Lo, C. W. (2004) Connexins and cell signaling in development and disease. Annu. Rev. Cell Dev. Biol. **20**, 811–838
6 Jordan, K., Solan, J. L., Dominguez, M., Sia, M., Hand, A., Lampe, P. D. and Laird, D. W. (1999) Trafficking, assembly, and function of a connexin43-green fluorescent protein chimera in live mammalian cells. Mol. Biol. Cell **10**, 2033–2050
7 Lopez, P., Balicki, D., Buehler, L. K., Falk, M. M. and Chen, S. C. (2001) Distribution and dynamics of gap junction channels revealed in living cells. Cell Commun. Adhes. **8**, 237–242
8 Gaietta, G., Deerinck, T. J., Adams, S. R., Bouwer, J., Tour, O., Laird, D. W., Sosinsky, G. E., Tsien, R. Y. and Ellisman, M. H. (2002) Multicolor and electron microscopic imaging of connexin trafficking. Science **296**, 503–507
9 Lauf, U., Giepmans, B. N., Lopez, P., Braconnot, S., Chen, S. C. and Falk, M. M. (2002) Dynamic trafficking and delivery of connexins to the plasma membrane and accretion to gap junctions in living cells. Proc. Natl. Acad. Sci. U.S.A. **99**, 10446–10451
10 Crow, D. S., Beyer, E. C., Paul, D. L., Kobe, S. S. and Lau, A. F. (1990) Phosphorylation of connexin43 gap junction protein in uninfected and Rous sarcoma virus-transformed mammalian fibroblasts. Mol. Cell. Biol. **10**, 1754–1763
11 Fallon, R. F. and Goodenough, D. A. (1981) Five-hour half-life of mouse liver gap-junction protein. J. Cell Biol. **90**, 521–526
12 Laird, D. W., Puranam, K. L. and Revel, J. P. (1991) Turnover and phosphorylation dynamics of connexin43 gap junction protein in cultured cardiac myocytes. Biochem. J. **273**, 67–72
13 Traub, O., Look, J., Dermietzel, R., Brummer, F., Hulser, D. and Willecke, K. (1989) Comparative characterization of the 21-kD and 26-kD gap junction proteins in murine liver and cultured hepatocytes. J. Cell Biol. **108**, 1039–1051
14 Berthoud, V. M., Minogue, P. J., Laing, J. G. and Beyer, E. C. (2004) Pathways for degradation of connexins and gap junctions. Cardiovasc. Res. **62**, 256–267
15 Laird, D. W. (1996) The life cycle of a connexin: gap junction formation, removal, and degradation. J. Bioenerg. Biomembr. **28**, 311–318
16 Musil, L. S., Le, A. C., VanSlyke, J. K. and Roberts, L. M. (2000) Regulation of connexin degradation as a mechanism to increase gap junction assembly and function. J. Biol. Chem. **275**, 25207–25215
17 Jordan, K., Chodock, R., Hand, A. R. and Laird, D. W. (2001) The origin of annular junctions: a mechanism of gap junction internalization. J. Cell Sci. **114**, 763–773
18 Risinger, M. A. and Larsen, W. J. (1983) Interaction of filipin with junctional membrane at different stages of the junction's life history. Tissue Cell **15**, 1–15
19 Vaughan, D. K. and Lasater, E. M. (1990) Renewal of electrotonic synapses in teleost retinal horizontal cells. J. Comp. Neurol. **299**, 364–374
20 Larsen, W. J. and Hai, N. (1978) Origin and fate of cytoplasmic gap junctional vesicles in rabbit granulosa cells. Tissue Cell **10**, 585–598
21 Mazet, F., Wittenberg, B. A. and Spray, D. C. (1985) Fate of intercellular junctions in isolated adult rat cardiac cells. Circ. Res. **56**, 195–204
22 Severs, N. J., Shovel, K. S., Slade, A. M., Powell, T., Twist, V. W. and Green, C. R. (1989) Fate of gap junctions in isolated adult mammalian cardiomyocytes. Circ. Res. **65**, 22–42
23 Sohl, G. and Willecke, K. (2003) An update on connexin genes and their nomenclature in mouse and man. Cell Commun. Adhes. **10**, 173–180
24 Rose, B., Mehta, P. P. and Loewenstein, W. R. (1993) Gap-junction protein gene suppresses tumorigenicity. Carcinogenesis **14**, 1073–1075
25 Shao, Q., Wang, H., McLachlan, E., Veitch, G. I. and Laird, D. W. (2005) Down-regulation of Cx43 by retroviral delivery of small interfering RNA promotes an aggressive breast cancer cell phenotype. Cancer Res. **65**, 2705–2711
26 Berthoud, V. M., Rook, M. B., Traub, O., Hertzberg, E. L. and Saez, J. C. (1993) On the mechanisms of cell uncoupling induced by a tumor promoter phorbol ester in clone 9 cells, a rat liver epithelial cell line. Eur. J. Cell Biol. **62**, 384–396
27 Lampe, P. D., TenBroek, E. M., Burt, J. M., Kurata, W. E., Johnson, R. G. and Lau, A. F. (2000) Phosphorylation of connexin43 on serine368 by protein kinase C regulates gap junctional communication. J. Cell Biol. **149**, 1503–1512
28 Rivedal, E., Yamasaki, H. and Sanner, T. (1994) Inhibition of gap junctional intercellular communication in Syrian hamster embryo cells by TPA, retinoic acid and DDT. Carcinogenesis **15**, 689–694
29 Rivedal, E. and Leithe, E. (2005) Connexin43 synthesis, phosphorylation, and degradation in regulation of transient inhibition of gap junction intercellular communication by the phorbol ester TPA in rat liver epithelial cells. Exp. Cell Res. **302**, 143–152
30 Leithe, E. and Rivedal, E. (2004) Ubiquitination and down-regulation of gap junction protein connexin-43 in response to 12-O-tetradecanoylphorbol 13-acetate treatment. J. Biol. Chem. **279**, 50089–50096
31 Oh, S. Y., Grupen, C. G. and Murray, A. W. (1991) Phorbol ester induces phosphorylation and down-regulation of connexin 43 in WB cells. Biochim. Biophys. Acta **1094**, 243–245
32 Lampe, P. D. (1994) Analyzing phorbol ester effects on gap junctional communication: a dramatic inhibition of assembly. J. Cell Biol. **127**, 1895–1905
33 Rivedal, E., Mollerup, S., Haugen, A. and Vikhamar, G. (1996) Modulation of gap junctional intercellular communication by EGF in human kidney epithelial cells. Carcinogenesis **17**, 2321–2328

34 Asamoto, M., Oyamada, M., el Aoumari, A., Gros, D. and Yamasaki, H. (1991) Molecular mechanisms of TPA-mediated inhibition of gap-junctional intercellular communication: evidence for action on the assembly or function but not the expression of connexin 43 in rat liver epithelial cells. Mol. Carcinog. **4**, 322–327
35 Montesano, R., Drevon, C., Kuroki, T., Saint, V. L., Handleman, S., Sanford, K. K., DeFeo, D. and Weinstein, I. B. (1977) Test for malignant transformation of rat liver cells in culture: cytology, growth in soft agar, and production of plasminogen activator. J. Natl. Cancer Inst. **59**, 1651–1658
36 Leithe, E., Cruciani, V., Sanner, T., Mikalsen, S. O. and Rivedal, E. (2003) Recovery of gap junctional intercellular communication after phorbol ester treatment requires proteasomal degradation of protein kinase C. Carcinogenesis **24**, 1239–1245
37 Opsahl, H. and Rivedal, E. (2000) Quantitative determination of gap junction intercellular communication by scrape loading and image analysis. Cell Adhes. Commun. **7**, 367–375
38 Slot, J. W. and Geuze, H. J. (1985) A new method of preparing gold probes for multiple-labeling cytochemistry. Eur. J. Cell Biol. **38**, 87–93
39 Horisberger, M. and Rosset, J. (1977) Colloidal gold, a useful marker for transmission and scanning electron microscopy. J. Histochem. Cytochem. **25**, 295–305
40 Slot, J. W., Geuze, H. J., Gigengack, S., Lienhard, G. E. and James, D. E. (1991) Immuno-localization of the insulin regulatable glucose transporter in brown adipose tissue of the rat. J. Cell Biol. **113**, 123–135
41 Simonsen, A., Lippe, R., Christoforidis, S., Gaullier, J. M., Brech, A., Callaghan, J., Toh, B. H., Murphy, C., Zerial, M. and Stenmark, H. (1998) EEA1 links PI(3)K function to Rab5 regulation of endosome fusion. Nature (London) **394**, 494–498
42 Miaczynska, M. and Zerial, M. (2002) Mosaic organization of the endocytic pathway. Exp. Cell Res. **272**, 8–14
43 Escola, J. M., Kleijmeer, M. J., Stoorvogel, W., Griffith, J. M., Yoshie, O. and Geuze, H. J. (1998) Selective enrichment of tetraspan proteins on the internal vesicles of multivesicular endosomes and on exosomes secreted by human B-lymphocytes. J. Biol. Chem. **273**, 20121–20127
44 Pillay, C. S., Elliott, E. and Dennison, C. (2002) Endolysosomal proteolysis and its regulation. Biochem. J. **363**, 417–429
45 Leithe, E. and Rivedal, E. (2004) Epidermal growth factor regulates ubiquitination, internalization and proteasome-dependent degradation of connexin43. J. Cell Sci. **117**, 1211–1220
46 Bright, N. A., Reaves, B. J., Mullock, B. M. and Luzio, J. P. (1997) Dense core lysosomes can fuse with late endosomes and are re-formed from the resultant hybrid organelles. J. Cell Sci. **110**, 2027–2040
47 Sachse, M., Ramm, G., Strous, G. and Klumperman, J. (2002) Endosomes: multipurpose designs for integrating housekeeping and specialized tasks. Histochem. Cell Biol. **117**, 91–104
48 Raiborg, C., Bache, K. G., Gillooly, D. J., Madshus, I. H., Stang, E. and Stenmark, H. (2002) Hrs sorts ubiquitinated proteins into clathrin-coated microdomains of early endosomes. Nat. Cell Biol. **4**, 394–398
49 Schmid, S. L., Fuchs, R., Male, P. and Mellman, I. (1988) Two distinct subpopulations of endosomes involved in membrane recycling and transport to lysosomes. Cell (Cambridge, Mass.) **52**, 73–83
50 Griffiths, G., Back, R. and Marsh, M. (1989) A quantitative analysis of the endocytic pathway in baby hamster kidney cells. J. Cell Biol. **109**, 2703–2720
51 Lampe, P. D. and Lau, A. F. (2000) Regulation of gap junctions by phosphorylation of connexins. Arch. Biochem. Biophys. **384**, 205–215
52 Drose, S. and Altendorf, K. (1997) Bafilomycins and concanamycins as inhibitors of V-ATPases and P-ATPases. J. Exp. Biol. **200**, 1–8
53 Saito, T., Schlegel, R., Andresson, T., Yuge, L., Yamamoto, M. and Yamasaki, H. (1998) Induction of cell transformation by mutated 16K vacuolar H^+-atpase (ductin) is accompanied by down-regulation of gap junctional intercellular communication and translocation of connexin 43 in NIH3T3 cells. Oncogene **17**, 1673–1680
54 Le, T. L., Yap, A. S. and Stow, J. L. (1999) Recycling of E-cadherin: a potential mechanism for regulating cadherin dynamics. J. Cell Biol. **146**, 219–232
55 Segretain, D., Decrouy, X., Dompierre, J., Escalier, D., Rahman, N., Fiorini, C., Mograbi, B., Siffroi, J. P., Huhtaniemi, I., Fenichel, P. et al. (2003) Sequestration of connexin43 in the early endosomes: an early event of Leydig cell tumor progression. Mol. Carcinog. **38**, 179–187

Received 26 April 2005/22 July 2005; accepted 15 September 2005
Published as BJ Immediate Publication 15 September 2005, doi:10.1042/BJ20050674